Chapter 67
Temperature and Strain Characteristic Analysis of Fiber Bragg Grating Sensor

Bing Bai, Yubin Guo, Xiaohui Zhao, Jiayu Huo and Tiegang Sun

Abstract A novel method is proposed to simulate temperature and strain characteristic of fiber Bragg grating (FBG) sensor with OptiGrating software, whose temperature characteristic is investigated experimentally with FBG sensing system based on broadband source one step further, both the simulation and experiment results show that the Bragg wavelength shift is linearly proportional to uniform temperature distribution. The parameters of FBG sensing system based on fiber ring laser have been optimized for good sensing performance, high signal-to-noise ratio (SNR) and powerful multiplexing capacity indicate its effectiveness and reliability in the application of long-haul sensing system.

Keywords Fiber bragg grating sensor · FBG sensing system · Fiber ring laser

67.1 Introduction

With the rapid development of photonic technology, optical fiber sensors play an important role in detecting outside information of nature. The fiber Bragg grating sensors have enormous potential in the application field of fiber-optic sensors as the result of immunity to electromagnetic interference, high sensitivity, small size, light weight and low cost [1–5]. The trial and error approach during fiber optical grating manufacturing process is extremely slow, expensive and unreliable, an

B. Bai · Y. Guo (✉) · X. Zhao · J. Huo · T. Sun
College of Communication Engineering, Jilin University, 5372 Nanhu Road, ChangChun, Jilin province, China

T. Sun
e-mail: suntieg@163.com

W. Lu et al. (eds.), *Proceedings of the 2012 International Conference on Information Technology and Software Engineering*, Lecture Notes in Electrical Engineering 210, DOI: 10.1007/978-3-642-34528-9_67,

appropriate fiber optical grating design and modeling software will help it develop towards an optimized production.

The essence of fiber grating sensor signal demodulation system is real-time monitoring of reflection spectrum from the sensing nodes, and analyses Bragg wavelength shift due to outside environment through the signal processing technology, and how to identify and measure a bunch of different wavelengths among reflected light is essential to wavelength demodulation and sensing grating addressing [6–9]. In order to realize Bragg wavelength shift detection, several optical fiber sensor signal interrogation techniques according to FBG sensor application situations have been proposed, including interrogation schemes based on a matched grating filter [10–12], an edge filter [13], a tunable F–P filter [14], an unbalanced M-Z interferometer [15], an unbalanced Michelson interferometer [16, 17], etc.

In this paper, OptiGrating software is adopted to simulate Bragg wavelength shift due to uniform temperature distribution and uniform strain distribution of the FBG sensor and its temperature characteristic is investigated based on broadband source/narrowband filter configuration. Operating principle is analyzed theoretically and sensing performance is investigated experimentally in fiber sensing system based on fiber ring laser [18, 19].

67.2 Fiber Bragg Grating Sensor

Simulation principle of OptiGrating is based on mode coupling theory, which is calculated by the Transfer Matrix Method, the Bragg wavelength and the FWHM bandwidth of the fiber grating can be given by:

$$\lambda_{\mathrm{B}} = 2\mathrm{n}_{\mathrm{eff}}\Lambda \tag{67.1}$$

$$\Delta\lambda_{\mathrm{FWHM}} = \lambda_{\mathrm{B}}\mathrm{S} \times \sqrt{\left[\left(\frac{\partial n}{2n}\right)^2 + \left(\frac{\Lambda}{L}\right)^2\right]} \tag{67.2}$$

Where the Bragg wavelength λ_{B} is 1549.38 nm, grating period Λ is 0.5345626 μm, and the length of fiber grating L is 50,000 μm, $\mathrm{S} = (\mathrm{k}^2 - \partial\beta^2)^{1/2}$, ∂n is the maximum range of refractive index.

The fiber Bragg grating shape is sinusoidal, average index is uniform. There is no chirp in the grating period, it is apodized by Gaussian function, and index modulation value is 0.00038. In addition, the sensors option needs to be checked in the grating manager dialog box. The FBG sensor is a narrowband optical filter, incident light who meet the Bragg conditions would be reflected back into the fiber in the opposite direction, transmission and reflection spectrum of FBG sensor in the free condition is shown in Fig. 67.1, its FWHM bandwidth is 0.30 nm.

Temperature and strain will change the grating refractive index and the grating period, spectral response of the FBG sensor changes when applied temperature and

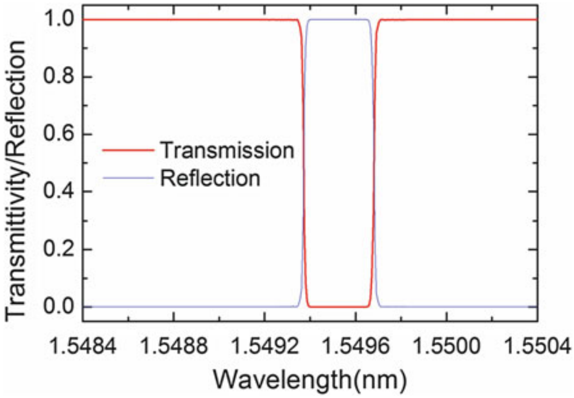

Fig. 67.1 Transmission and reflection spectrum of fiber Bragg grating sensor

strain distributions change. Refractive index change and grating period change caused by the temperature and strain contribute to the Bragg wavelength shift $\Delta\lambda_{BT}$ and $\Delta\lambda_{B\varepsilon}$.

$$\frac{\Delta\lambda_{BT}}{\lambda_B} = (\alpha + \xi) \cdot \Delta T \tag{67.3}$$

$$\frac{\Delta\lambda_{B\varepsilon}}{\lambda_B} = \left(1 - \frac{n^2}{2[P_{12} - v(P_{11} - P_{12})]}\right)\Delta\varepsilon \tag{67.4}$$

Where thermal-expansion coefficient α is 5.5e − 007/°C, thermal-optic coefficient ξ is 8.3e − 006/°C, strain-optical tensor P_{11} and P_{12} entered are 0.121 and 0.27 respectively, and Poisson ratio v is 0.17.

Uniform temperature distribution and uniform strain distribution are applied to the FBG sensor respectively, Bragg wavelength shift will be detected due to the temperature change or strain change, the problem of cross sensitivity is not included within the scope of the paper. The temperature varies from 25 to 45 °C with a step of 1 °C, Fig. 67.2 a shows Bragg wavelength shift due to uniform temperature change. The strain increases from 0 to 150 με with a step of 5 με Fig. 67.2b shows Bragg wavelength shift due to uniform strain change. As can be seen in Fig. 67.2, the Bragg wavelength shift is linear with uniform temperature change or uniform strain change, Bragg wavelength moves to longer wavelength as temperature increases or strain increases. The estimated linear regression models are stated: y = 0.01367*x + 1,549.03887 and y = 0.00101*x + 1549.37963, whose correlation coefficients are 0.99979 and 0.99928 respectively, temperature sensitivity obtained is 13.67 pm/°C and strain sensitivity obtained is 1.01 pm/με.

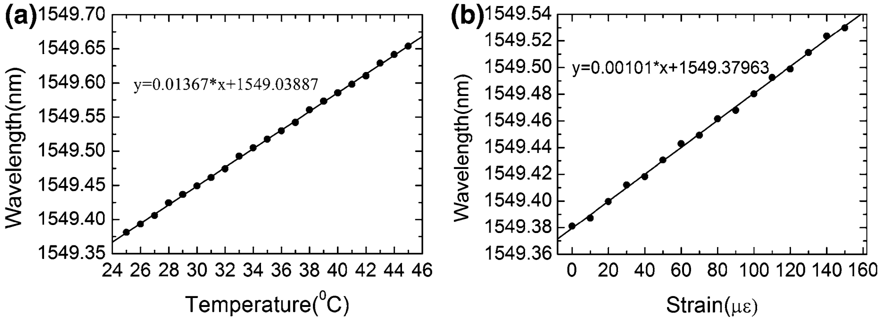

Fig. 67.2 **a** Relation between Bragg wavelength shift and uniform temperature distribution. **b** Relation between Bragg wavelength shift and uniform strain distribution

67.3 FBG Sensing System

67.3.1 Broadband Source

The schematic diagram of the basic FBG sensing system configuration based on broadband source (BBS) is shown in Fig. 67.3. The light source for FBG sensing system is a broadband source, narrowband scanning filter (SF) spectrum convolutes with reflection spectrum of FBG sensor. The maximum convolution results reach when reflection spectrum of FBG sensor and SF spectrum match, a measured reflection curve will be obtained, Bragg wavelength relates to outside temperature information.

In the experiment, the free termination have been immersed in refractive index matching gel (IMG) to avoid undesired reflections [20], and isolator (ISO) is introduced to protect BBS. In addition, the resolution of temperature cabinet is limited to 1 °C. The relation between the Bragg wavelength shift and temperature distribution is measured based on broadband source/narrowband filter configuration. According to Bragg wavelength shift and temperature change data, a measured reflection curve is shown in Fig. 67.4. The estimated linear regression model is stated: $y = 0.01313*x + 1549.04699$, whose correlation coefficient is 0.99515, temperature sensitivity obtained is 13.13 pm/°C. The simulation and experimental results are consistent with each other, which prove that the Bragg wavelength is linear with the temperature change.

Fig. 67.3 FBG sensing system based on broadband source

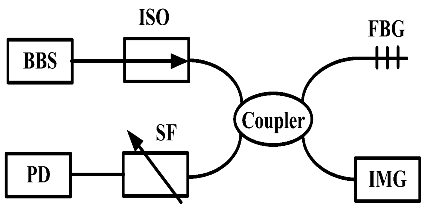

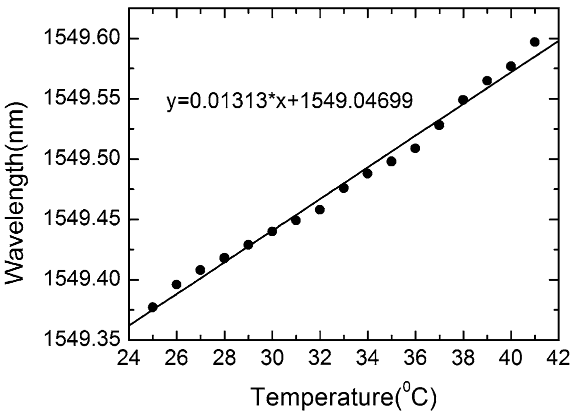

Fig. 67.4 Relation between Bragg wavelength shift and uniform temperature distribution

67.3.2 Fiber Ring Laser

Based on the simulation and experiment investigation on FBG sensor's sensing characteristic, a FBG sensing system scheme based on fiber ring laser is designed, as shown in Fig. 67.5. In order to choose the lasing wavelength in the waveband 1526.438–1564.679 nm, a dielectric thin-film filter (DTF) is introduced. The erbium doped fiber (EDF) makes up one end of the ring cavity while FBG sensors composes the other end. The Bragg wavelengths are different from each other, but they are all located in the gain bandwidth of EDF. Fiber sensing system chooses a lasing wavelength when the transmission window of DTF matches the wavelength of FBG sensor's reflection spectrum from remote sensing node, then real-time monitoring for Bragg wavelength shift has been realized.

The parameters of FBG sensing system are optimized in order to improve sensing performance, then 1.8 m-long EDF is chosen as gain medium whose peak absorption coefficient is 24 dB/m at 1,530 nm. 2×2 coupler with split ratio of 90:10 is incorporated into the ring cavity instead of 1×2 coupler and circulator, which decreases system loss, complexity and cost. A FBG sensor is located at

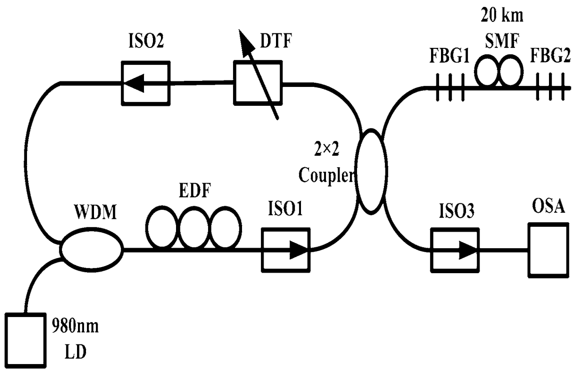

Fig. 67.5 FBG sensing system based on fiber ring laser

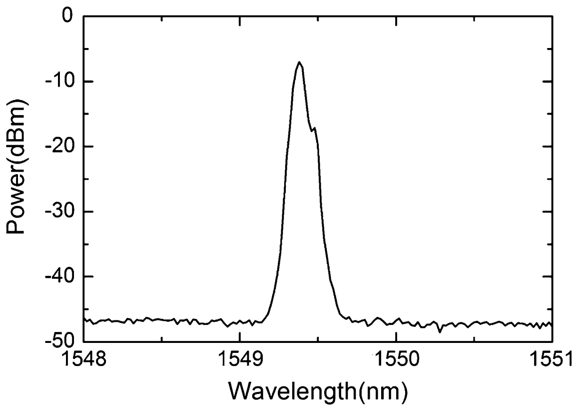

Fig. 67.6 A 20 km FBG sensor interrogation signal spectrum

20 km sensing node, interrogation signal taken from 90 % output of 2 × 2 coupler is measured by optical spectrum analyzer (OSA). As can be seen from Fig. 67.6, the relative peak power is −7.03 dBm for a pump power of 100 mW, the side mode suppression ratio (SMSR) is lager than 38 dB, and 3 dB bandwidth is less than 0.08 nm.

The FBG sensing system based on broadband source suffers from a low SNR as result of the low power spectrum intensity of broadband source, and as is known that the SNR declines as the distance increases. However, FBG sensing system based on fiber ring laser enhances the SNR and provides a higher output power with a narrow spectral width. Even though the back-reflected signal degrades along 20 km fiber link, the SNR of the interrogation signal remains high, which indicates its demodulation performance is good. Because of the wide tuning range of DTF, FBG sensing system based on fiber ring laser is capable of supporting 18 FBG sensors with 2 nm per bandwidth interval at least, which means its multiplexing capacity is powerful.

67.4 Conclusion

Both strain and temperature characteristic of FBG sensor are simulated incorporating OptiGrating software, temperature characteristic is investigated experimentally. Both simulation and experimental results are consistent with each other, the Bragg wavelength shift is linearly proportion to uniform temperature distribution. Based on simulation and experimental research on FBG sensor's sensing characteristic, we demonstrate an optimized FBG sensing system configuration based on fiber ring laser. High SNR of a 20 km FBG sensor interrogation signal and powerful multiplexing capacity of FBG sensing system indicate good sensing performance, which have theoretical significance to the high precision, long-haul efforts and extremely sensitive fiber sensing market development in future.

References

1. Bazzo JP, Lukasievicz T, Vogt M et al (2012) Thermal characteristics analysis of an IGBT using a fiber Bragg grating. Opt Laser Eng 50:99–103
2. Childs P, Wong ACL, Yan BB et al (2010) A review of spectrally coded multiplexing techniques for fibre grating sensor systems. Meas Sci Technol 21:094007
3. Luyckx G, Voet E, Lammens N et al (2011) Strain measurements of composite laminates with embedded fibre Bragg gratings: criticism and opportunities for research. IEEE Sens J 11:384–408
4. Liu QW, Tomochika T, Zuyuan H (2011) Realization of nano static strain sensing with fiber Bragg gratings interrogated by narrow linewidth tunable lasers. Opt Express 19(21):20214
5. Wang YP, Wang M, Huang XQ (2011) Spectral characterization of polarization dependent loss of locally pressed fiber Bragg grating. Opt Express 19(25):25535–25544
6. Li RM, Yu YL, Shum P (2011) Addressing fiber Bragg grating sensors with wavelength-swept pulse fiber laser and analog electrical switch. Opt Commun 284:1561–1564
7. Liu WJ, Li M, Wang C (2011) Real time interrogation of a linearly chirped fiber Bragg grating sensor. J Lightwave Technol 29(9):1239–1247
8. Wang C, Yao JP (2011) Ultrafast and ultrahigh-resolution interrogation of a fiber Bragg grating sensor based on interferometric temporal spectroscopy. J Lightwave Technol 29(19): 2927–2933
9. Yang MW, Liao CR (2011) Fiber Bragg grating with micro-holes for simultaneous and independent refractive index and temperature sensing. IEEE Photon Technol Lett 23(20):1511–1513
10. Jiang BQ, Zhao JL, Qin C et al (2011) An optimized strain demodulation method based on dynamic double matched fiber Bragg grating filtering. Opt Laser Eng 49:415–418
11. Zhan YG, Yu MH, Pei JC et al (2010) A linearity interrogation technique with enlarged dynamic range for fiber Bragg grating sensing. Opt Commun 283:3428–3433
12. Zou HB, Liang DK, Zeng J (2012) Dynamic strain measurement using two wavelength-matched fiber Bragg grating sensors interrogated by a cascaded long-period fiber grating. Opt Laser Eng 50:199–203
13. Navneet SA, Kaler RS (2011) Fiber Bragg grating interrogator using edge filtering technique with microbend loss error mitigation. Opt 122(9):796–798
14. Kuo ST, Peng PC, Kao MS (2011) Tunable erbium-doped fiber ring laser with signal-averaging function for fiber-optic sensing applications. Laser Phys 21(1):188–190
15. Liao CR, Wang Y, Wang DN et al (2010) Fiber in-line Mach-Zehnder interferometer embedded in FBG for simultaneous refractive index and temperature measurement. IEEE Photon Technol Lett 22(22):1686–1688
16. Amaral LMN, Frazão O, Santos JL et al (2011) Fiber-optic inclinometer based on taper Michelson interferometer. IEEE Sens J 11(9):1811–1814
17. Min JW, Yao BL, Gao P (2010) Parallel phase-shifting interferometry based on Michelson-like architecture. Appl Opt 49(34):6612–6616
18. Tsuda H (2010) Fiber Bragg grating vibration-sensing system, insensitive to Bragg wavelength and employing fiber ring laser. Opt Lett 35(14):2349–2351
19. Gan JL, Hao YQ, Ye Q et al (2011) High spatial resolution distributed strain sensor based on linear chirped fiber Bragg grating and fiber loop ringdown spectroscopy. Opt Lett 36(6): 879–881
20. Quintela MA, Herrera RAP, Canales I et al (2010) Stabilization of dual-wavelength erbium-doped fiber ring lasers by single-mode operation. IEEE Photon Technol Lett 22(6):368–370